A conserved salt bridge critical for $GABA_A$ receptor function and loop C dynamics

Srinivasan P. Venkatachalan and Cynthia Czajkowski*

Department of Physiology, University of Wisconsin–Madison, 601 Science Drive, Madison, WI 53711

Edited by Arthur Karlin, Columbia University College of Physicians and Surgeons, New York, NY, and approved July 11, 2008 (received for review February 25, 2008)

Chemical signaling in the brain involves rapid opening and closing of ligand gated ion channels (LGICs). LGICs are allosteric membrane proteins that transition between multiple conformational states (closed, open, and desensitized) in response to ligand binding. While structural models of cys-loop LGICs have been recently developed, our understanding of the protein movements underlying these conformational transitions is limited. Neurotransmitter binding is believed to initiate an inward capping movement of the loop C region of the ligand-binding site, which ultimately triggers channel gating. Here, we identify a critical intrasubunit salt bridge between conserved charged residues (βE153, βK196) in the $GABA_A$ receptor ($GABA_AR$) that is involved in regulating loop C position. Charge reversals (E153K, K196E) increased the EC_{50} for GABA and for the allosteric activators pentobarbital (PB) and propofol indicating that these residues are critical for channel activation, and charge swap (E153K-K196E) significantly rescued receptor function suggesting a functional electrostatic interaction. Mutant cycle analysis of alanine substitutions indicated that E153 and K196 are energetically coupled. By monitoring disulfide bond formation between cysteines substituted at these positions (E153C-K196C), we probed the mobility of loop C in resting and ligand-bound states. Disulfide bond formation was significantly reduced in the presence of GABA or PB suggesting that agonist activation of the $GABA_AR$ proceeds via restricting loop C mobility.

disulfide trapping | electrostatic | ligand-gated ion channel | mutant cycle

Even though significant strides have been made in our understanding of the structures of members of the cys-loop family of LGICs, the structural elements and protein movements that couple neurotransmitter binding to channel opening are only beginning to be elucidated (1). Members of the cys-loop family of receptors include the prototypical nicotinic acetylcholine receptor (nAChR), $GABA_AR$, the glycine receptor (GlyR) and the serotonin $5HT_3$ receptor ($5HT_3R$). For these receptors, binding of neurotransmitter in the extracellular ligand-binding domain results in a rapid cascade of protein rearrangements (in the submillisecond to millisecond timescale) (2) that ultimately leads to the opening of an intrinsic ion pore.

Much of our current structural knowledge of these nanomachines comes from the crystal structure of the related molluscan acetylcholine binding protein (AChBP), which shares sequence homology to the extracellular ligand-binding domain of these receptors (3) and from the 4 Å cryo-electron microscopic images of the nAChR in the closed state (4). These static snapshots, however, cannot completely describe the protein movements involved in coupling neurotransmitter binding to channel gating. Molecular dynamic simulations, fluorescence studies using tethered flurophores, and a hydrogen-deuterium exchange study have suggested that the loop C region of the neurotransmitter binding site (Fig. 1*A*) located between beta strands 9 (β9) and 10 (β10), is dynamic (5–7). Presently, it is believed that neurotransmitter binding triggers an inward capping motion of loop C over the agonist, which then leads to channel opening via molecular interactions in the coupling interface (8–10). The molecular forces that control the positioning and stabilization of loop C in agonist bound (open and desensitized) and unbound (resting) receptor states are relatively unknown. In the nAChR, it has been suggested that a triad of interacting residues near the periphery of the ACh binding site are involved in coupling movements in the binding site to the ion channel (11).

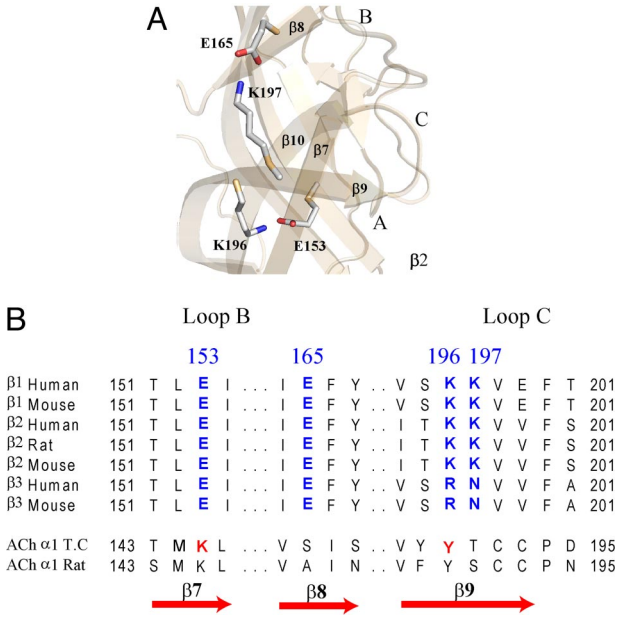

Fig. 1. Model of $GABA_AR$ extracellular N-terminal domain based on AChBP (ligand bound). (*A*) Charged residues in the β2 subunit (E153, E165, K196, and K197) that might be involved in regulating movement of loop C via electrostatic interactions are shown. Binding site loops A, B, and C are marked. (*B*) Sequences of various $GABA_AR$ β-subunits highlighting conserved charged residues (blue). Aligned residues in the nAChR α-subunit from *Torpedo californica* and *Rattus norvegicus* are also shown. Residues suggested to form a salt bridge important for stabilizing the open state of nAChR (Mukhtasimova *et al.*) (11) are colored red.

Here, we identify a salt bridge between βE153 and βK196 involved in positioning loop C and present evidence that this salt bridge is critical for GABA activation of the receptor. Moreover, using disulfide-trapping experiments, we demonstrate that in the unliganded resting state, the loop C region of the GABA binding site undergoes significant motion, and that GABA and PB slow this motion.

Results

Effects of Charge Reversals and Charge Swap on GABA Activation. On the basis of a homology model of the extracellular domain of the

Author contributions: S.P.V. and C.C. designed research; S.P.V. performed research; S.P.V. analyzed data; and S.P.V. and C.C. wrote the paper.

The authors declare no conflict of interest.

This article is a PNAS Direct Submission.

*To whom correspondence should be addressed. E-mail: czajkowski@physiology.wisc.edu.

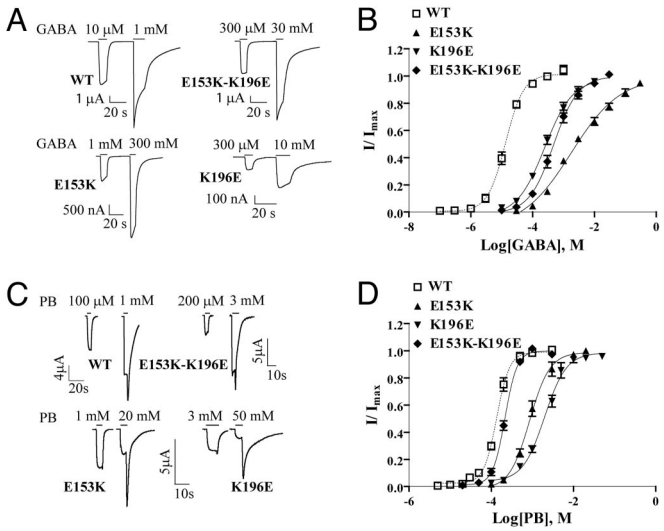

Fig. 2. GABA and PB concentration–response curves. (*A* and *C*) Representative GABA and PB currents from oocytes expressing WT $\alpha1\beta2\gamma2S$, $\alpha1\beta2E153K\gamma2S$, $\alpha1\beta2K196E\gamma2S$, and $\alpha1\beta2E153K\text{-}K196E\gamma2S$ $GABA_A$Rs. (*B* and *D*) GABA and PB concentration-response curves from oocytes expressing $\alpha1\beta2\gamma2S$ (open squares, dashed line), $\alpha1\beta2E153K\gamma2S$ (filled triangles), $\alpha1\beta2K196E\gamma2S$ (inverted filled triangles), $\alpha1\beta2E153K\text{-}K196E\gamma2S$ (filled diamonds) receptors. Data points represent mean ± SEM from at least three experiments and at least two batches of oocytes. Data were fit by nonlinear regression analysis as described in *Materials and Methods*.

$GABA_A$R, we observed potential electrostatic interactions between charged amino acid residues on β7 (E153) and β9 (K196) and β8 (E165) and β9 (K197) (Fig. 1 *A* and *B*). Residues in similar positions on β7 and β9 in the nAChR (Fig. 1*B*) have been reported to interact (11). Because β9 forms part of the loop C region of the GABA binding site (Fig. 1*A*), we hypothesized that interactions between these residues might be involved in positioning and stabilizing loop C during receptor activation. To test our hypothesis, we disrupted the salt bridges by reversing the charges (βE153K, βE165K, βK196E, and βK197E) and also swapped the charges (βE153K-K196E and βE165K-K197E) to potentially restore the salt bridges. Oocytes expressing mutant and wild type (WT) $\alpha1\beta2\gamma2S$ $GABA_A$R's were functionally characterized using a two-electrode voltage clamp. All of the mutant β-subunits assembled into receptors that responded to GABA. Charge reversals at βE153 and βK196 increased GABA EC_{50} by 137- and 19-fold, respectively, as compared to WT (13.3 ± 1.5 μM) (Fig. 2 *A* and *B*; Table 1) whereas the charge reversals at βE165 and βK197 had little effect on GABA EC_{50} (Table 1). When the charges at βE153 and βK196 were swapped (βE153K-K196E), GABA EC_{50} was increased by only 37-fold. If the mutations at βE153 and βK196 acted independently, the effect of the double mutation should be additive and result in a 2600-fold increase in GABA EC_{50}.

Effects of Charge Reversals and Charge Swap on General Anesthetic Activation. PB is an allosteric modulator of the $GABA_A$R that binds at a site distinct from GABA (12). At high concentrations, PB can directly open the channel. The single channel conductances of $GABA_A$R's activated by PB and GABA are similar (13) suggesting that the open-state channel structures induced by their binding are alike. We hypothesized that if an interaction between βE153 and βK196 is important for stabilizing an open, activated state of the $GABA_A$R, then the ability of PB to gate the $GABA_A$R would also be altered by mutations at these positions. Charge reversals at βE153 and βK196 increased PB EC_{50} by 6- and 15-fold, respectively, as compared to WT (141 ± 10 μM) (Fig. 2 *C* and *D*, Table 1). When the charges were swapped (βE153K-K196E), PB EC_{50} was restored to near WT values (Fig. 2*D*, Table 1).

We also examined whether E153 and K196 were important for $GABA_A$R activation by the general anesthetic propofol. Charge reversals at βE153 and βK196 each decreased propofol apparent affinity, ≈7-fold (E153K, EC_{50} = 430 ± 18 μM, n = 4; K196E, 569 ± 122 μM, n = 5; *vs*. WT, 72 ± 34 μM, n = 2). Notably, the charge swap restored propofol EC_{50} to near WT values (46 ± 24 μM, n = 3). Rescue of PB and propofol EC_{50} with the charge swap argues against the mutations inducing global structural changes in the protein.

The effects of reversing the charges (βE165K, βK197E) and swapping the charges (βE165K-K197E) at βE165 and βK197 on the ability of PB to activate the $GABA_A$R were also tested. Similar to results obtained with GABA, these mutations had little effects on PB EC_{50} (Table 1) indicating that an interaction between βE165 and βK197, if present, is not important for PB or GABA activation of the $GABA_A$R.

Cysteine Substitutions and Modification with Charged MTS Reagents. To confirm the electrostatic nature of the interaction between βE153 and βK196, we examined the effects of inserting positive and negative charges at these positions in real-time. Initially, we neutralized the charges by introducing cysteine substitutions at

Table 1. Summary of GABA and PB concentration responses

Receptor	(EC_{50}, μM) GABA	n_H	mut/WT	N	ΔΔG kcal/mol	(EC_{50}, μM) PB	n_H	mut/WT	N	ΔΔG kcal/mol
WT	13.3 ± 1.5	1.5 ± 0.1	1	5		141 ± 10	2.9 ± 0.3	1	6	
E153A	1917 ± 549*	0.7 ± 0.1*	144	4		732 ± 29*	2.2 ± 0.1	5	3	
K196A	69 ± 12*	1.0 ± 0.1*	5	3		151 ± 9	2.0 ± 0.2	1	3	
E153A-K196A	1,031 ± 206*	0.9 ± 0.1*	78	5	−1.35 ± 0.19†	536 ± 90*	2.8 ± 0.4	4	3	−0.23 ± 0.07†
E153K	1820 ± 25*	0.6 ± 0.1*	137	4		873 ± 78*	1.9 ± 0.3	6	4	
K196E	258 ± 42*	0.9 ± 0.1*	19	6		2080 ± 243*	1.7 ± 0.2*	15	5	
E153K-K196E	489 ± 105*	1.1 ± 0.1	37	4	N.D.	216 ± 12*	2.9 ± 0.1	2	5	N.D.
E165K	6.3 ± 1.1	1.3 ± 0.1	0.5	4		160 ± 18	3.0 ± 0.4	1	5	
K197E	3.9 ± 0.9*	1.3 ± 0.1	0.3	5		149 ± 9	2.4 ± 0.2	1	4	
E165K-K197E	7.5 ± 2.8	1.0 ± 0.1*	0.6	4	N.D.	126 ± 21	2.4 ± 0.4	1	3	N.D.
E153C	1200 ± 105*	0.8 ± 0.2	90	4						
K196C	77 ± 5*	1.0 ± 0.2	6	3						
E153C-K196C	10 ± 4.5 mM*	0.5 ± 0.1*	750	3	N.D.					

Data are mean ± SEM for N experiments. GABA and PB EC_{50} values, Hill coefficients, and mutant/WT (mut/WT) EC_{50} ratios are indicated.
*Values are significantly different from WT, $P < 0.05$ (one-way ANOVA).
†Value is significantly different from 0 (one-sample t-test, $P < 0.05$). N.D., values not determined.

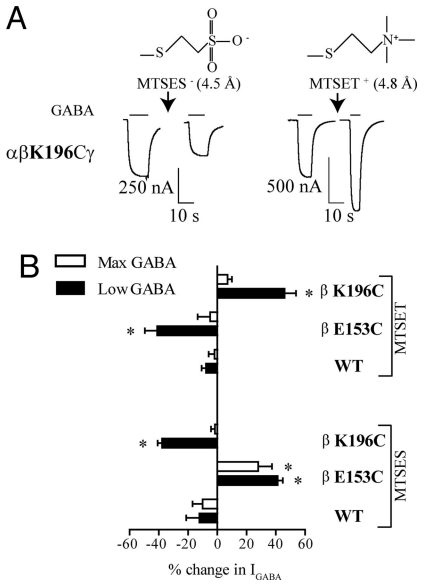

Fig. 3. Effects of MTS reagents on WT and mutant $GABA_A$Rs. (*A*) Structures and lengths of the MTS reagents that covalently modify an introduced cysteine and representative current traces from two different oocytes expressing $\alpha\beta$K196Cγ receptors before and after modification by charged MTS reagents are shown. Modification of $\alpha\beta$K196Cγ by a 2-min application of 2 mM $MTSET^+$ (arrow) enhances EC_{30-60} GABA current amplitude whereas modification using a 2-min application of 2 mM $MTSES^-$ (arrow) decreases EC_{30-60} GABA current amplitude. (*B*) Bar graph summary of the percentage of change (mean ± SEM) in low (EC_{30-60}) and max GABA current (I_{GABA}) amplitude after modification of WT and mutant (βE153C and βK196C) receptors with MTSET or MTSES. The percentage of change in I_{GABA} after MTS treatment is defined as: $[((I_{after}/I_{inital}) - 1) \times 100]$. Negative values represent a decrease in I_{GABA} after MTS reaction, whereas positive values represent an increase in I_{GABA}. *, values are significantly different from WT, $P < 0.05$ (one-way ANOVA).

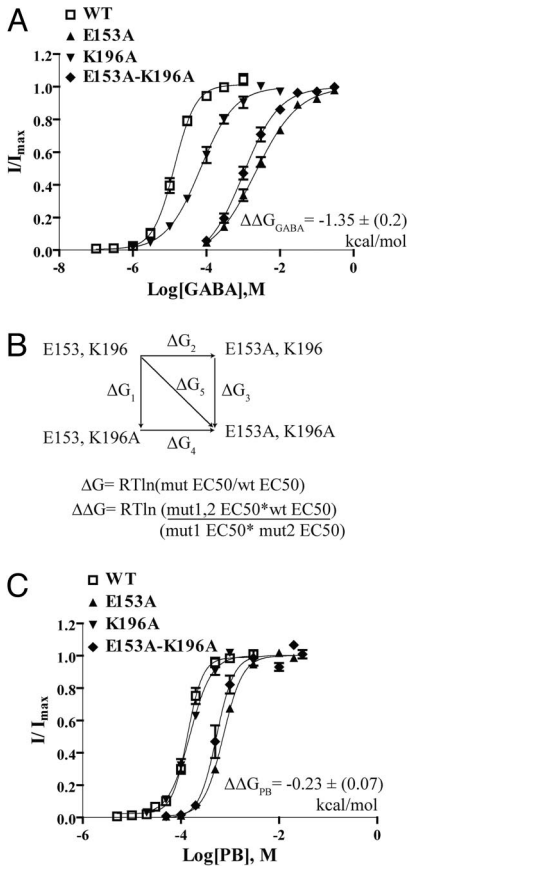

Fig. 4. Mutant cycle analysis indicates that βE153 and βK196 are energetically coupled. (*A* and *C*) GABA and PB dose-response curves for singly and doubly substituted alanines at βE153 and βK196. In each case, the double alanine mutant was as adversely affected as the most severely affected single alanine mutant indicating an interaction between βE153 and βK196. Interaction energy ($\Delta\Delta G$) in *A* and *C* is mean ± SEM. (*B*) Mutant cycle and equations for calculating change in free energy (ΔG) and the overall interaction energy ($\Delta\Delta G$) are indicated.

these positions (βE153C, βK196C). βE153C and βK196C increased GABA EC_{50} by 90- and 6-fold, respectively, as compared to WT (see Fig. 5*A* and Table 1).

We then examined the effects of modifying the substituted cysteines with a positively (MTSET) and a negatively (MTSES) charged sulfhydryl-reactive reagent. MTSET and MTSES are similar in molecular size (Fig. 3*A*) and have similar reaction mechanisms (14). Thus, differences in a cysteine mutant receptor's response following modification by these reagents can be directly attributed to adding different charges to the substituted cysteines. For WT receptors, MTSES and MTSET (2 mM, 2 min) had no significant effects on currents activated by EC_{30-60} (10 μM) and max GABA (10 mM) concentrations (<15%; Fig. 3*B*).

As expected, modification of βE153C with the negatively charged MTSES significantly increased current amplitudes in response to EC_{30-60} GABA (1 mM) by 41.3 ± 3.5% (Fig. 3*B*). Similarly, modification of βK196C with the positively charged MTSET significantly increased EC_{30-60} GABA (80 μM) current amplitudes by 46.1 ± 7.8%. Moreover, modification of βE153C with MTSET and modification of βK196C with MTSES significantly decreased current responses to EC_{30-60} GABA (Fig. 3*B*). An increase or decrease in I_{GABA} after MTS application can be attributed to a change in GABA apparent affinity (EC_{50}) and/or a change in maximal GABA response (I_{max}). Except for βE153C, MTS modifications had no effect on I_{max}. Modification of βE153C with MTSES significantly increased GABA (300 mM) I_{max} by 27.9 ± 9.5% (Fig. 3*B*), suggesting a change in channel gating or conductance. Because of βE153C's distance from the channel vestibule, a change in gating is the simplest explanation. Overall, removing the charges at E153 or K196 by cysteine substitution decreased $GABA_A$R activation whereas returning the negative charge at E153 and the positive charge at K196 restored function.

Nonadditive Effects of Salt Bridge Mutations. The nonadditivity of the effects of the double charge swap on GABA and PB EC_{50} values suggests that βE153 and βK196 interact. Mutant cycle analysis is routinely used to compute the interaction energy between sets of residues on the basis of the free energy change associated with a perturbation (15). For this analysis, the introduced mutations should remove the interaction under study without adding new interactions (16, 17). Thus, we neutralized E153 and K196 independently and together, by introducing alanines. If the residues do not interact then the change in free energy for the double mutant is equal to the sum of the changes in free energy of the two single mutations. If the residues are energetically coupled then the change in free energy for the double mutant would differ from the sum of the two single mutations (Fig. 4*B*).

Alanine substitutions of βE153 and βK196 increased GABA EC_{50} by 144- and 5-fold, respectively (Fig. 4*A*, Table 1). As expected for interacting residues, the GABA EC_{50} for the double alanine mutant (βE153A-K196A) was not the additive sum of the single mutants (Fig. 4*A*, Table 1). Mutant cycle analysis yielded a significant interaction energy of (−) 1.35 ± 0.2

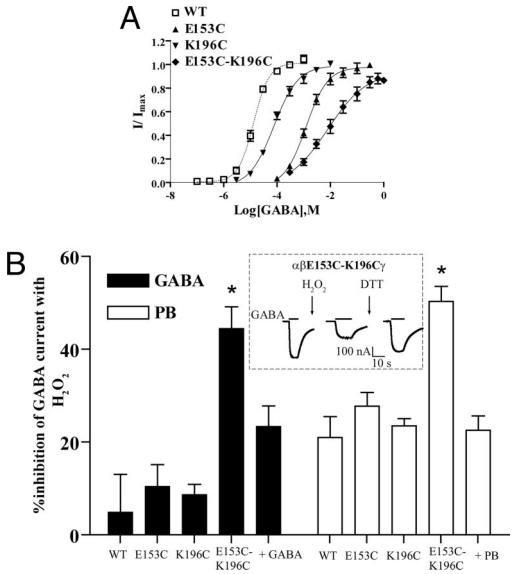

Fig. 5. Cross-linking indicates that βE153C and βK196C are spatially proximal and that agonist activation (GABA or PB) limits the mobility of loop C. (*A*) GABA concentration-response curves from oocytes expressing WT α1β2γ2S (open squares, dashed line), α1β2E153Cγ2S (filled triangles), α1β2K196Cγ2S (inverted filled triangles), and α1β2E153C-K196Cγ2S (filled diamonds) receptors. (*B*) Percentage of inhibition of I_{GABA} or I_{PB} for WT and mutant receptors after promoting cysteine cross-linking with 0.3% H_2O_2 for 3 min in the presence and absence of GABA or PB. Data are mean ± SEM from at least three experiments and at least two batches of oocytes. (*Inset*) Current traces from an oocyte expressing α1β2E153C-K196Cγ2S receptor during a cross-linking experiment. The inhibition of GABA current amplitude after application of 0.3% H_2O_2 is reversed by 10 mM DTT (3 min). *, values are significantly different from WT, $P < 0.05$ (one-way ANOVA).

kcal/mol. A similar analysis for PB activation yielded a weaker coupling energy of (−) 0.23 ± 0.07 kcal/mol (Fig. 4*C*, Table 1). The differences in the interaction energies for GABA and PB activation likely reflect the fact that GABA and PB bind to different regions of the receptor and trigger different activation pathways and movements (18).

Mutant cycle analysis was developed for analyzing two-state thermodynamic processes (19–21). The EC_{50} values used in our analysis are a composite of microscopic agonist binding and channel gating constants. This complicates the analysis and our ascribing whether the interaction influences agonist binding and/or gating. Nonetheless, the nonadditivity of the effects on GABA EC_{50} for the double-substitution mutations (charge swap and/or alanines) when compared to the single substitutions strongly suggests that βE153 and βK196 interact.

Disulfide Trapping. To probe the spatial proximity between βE153 and βK196 and their mobility, we tested the ability of cysteines introduced at βE153 and βK196 (βE153C-βK196C, Fig. 5*A* and Table 1) to form a disulfide bond. The maximum separation of cysteine beta-carbons (C^{β}-C^{β}) in a disulfide bond (-S-S-) is 4.6 Å (22). Factors affecting disulfide bond formation include sulfhydryl collision frequency and collision trajectory and the presence of an oxidizing environment (22). We used the oxidizing agent H_2O_2 (0.3%, 3 min) to promote disulfide bond formation. H_2O_2 had minimal effects on WT and single cysteine GABA EC_{50} currents (Fig. 5*B*) but significantly reduced GABA induced current by 44.4 ± 4.7% ($n = 7$) for the double cysteine mutant receptor (βE153C-βK196C). Subsequent treatment with the disulfide reducing reagent DTT (10 mM, 3 min) regenerated ≈70–80% of the initial GABA current (*inset*, Fig. 5*B*) providing strong evidence that the H_2O_2 induced current inhibition is caused by a disulfide bond between βE153C and βK196C. For a subset of oocytes expressing βE153C-βK196C, application of DTT to naïve oocytes significantly increased EC_{50} GABA current amplitudes (data not shown) suggesting that under certain conditions the two cysteines are spontaneously crosslinked. The variability in observing spontaneous disulfide bond formation between βE153C and βK196C is likely because of differences in the redox environment of different batches of oocytes (23).

Disulfide bond formation induced by H_2O_2 between βE153C and βK196C reduced GABA gated current and likely traps loop C in a position not favorable for receptor activation. To test whether disulfide trapping β9 close to β7 was also detrimental to PB gating of the receptor, we tested the effects of H_2O_2 on EC_{50} PB (1 mM) induced currents (Fig. 4*B*). Similar to the results obtained with GABA, H_2O_2 significantly decreased PB-gated currents by 50.2 ± 3.2% ($n = 9$) for the double cysteine mutant receptor (βE153C-βK196C) but had small effects on WT and single-mutant receptors (Fig. 5*B*). The larger effects that H_2O_2 had on PB currents compared to GABA currents elicited from WT receptors is likely because of differences in the oxidative sensitivity of the individual structural elements that make up their distinct activation trajectories.

To examine whether $GABA_AR$ activation by GABA or PB changes the distance/relative orientation/thermal motion of βE153C on β7 and βK196C on β9 we tested the ability of H_2O_2 to promote disulfide bond formation in the presence of GABA (300 mM) or PB (1 mM). The inhibition of GABA current responses induced by H_2O_2 was significantly decreased in the presence of GABA (23.3 ± 4.4%; $n = 4$ *vs*. 44.4 ± 4.7%; $n = 7$ in the absence of GABA, Fig. 5*B*) suggesting that GABA blocks disulfide bond formation between βE153C and βK196C. The decrease in disulfide bond formation could be because of steric block from GABA itself or to local structural movements triggered by GABA binding. To try and distinguish between these possibilities, we examined whether the presence of PB would also decrease H_2O_2 induced inhibition of PB activated currents. PB significantly reduced disulfide bond formation (22.5 ± 3.1%; $n = 5$ *vs*. 50.2 ± 3.2%; $n = 9$ in the absence of PB, Fig. 5*B*). Overall, the data demonstrate that disulfide bond formation between βE153C and βK196C is decreased in the presence of GABA and PB. The reduced levels of crosslinking in the ligand-bound states suggest that $GABA_AR$ activation changes the position of loop C. Moreover, the data suggests that binding of PB in the presumed transmembrane domain (24–26) triggers movement in the receptor that can be backpropagated to the GABA binding pocket.

Discussion

Because neurotransmitter binding to LGICs triggers channel opening within milliseconds, the underlying protein movements must happen on an even faster timescale. The breaking and forming of salt bridges is estimated to occur in nanoseconds making them ideal for participating in this process (27, 28). Here, we provide evidence that a salt bridge between βE153 and βK196 located on β7 and β9 of the $GABA_AR$ is important for regulating loop C movement.

Intrasubunit Salt Bridge Critical for $GABA_AR$ Activation. Several lines of evidence indicate that E153-K196 forms a functionally important salt bridge in the $GABA_AR$. Charge reversal and charge neutralization resulted in large rightward shifts in GABA EC_{50} values (Table 1). Modification of K196C with positively charged MTSET and E153C with negatively charged MTSES restored $GABA_AR$ function whereas modifications with oppositely charged MTS reagents reduced $GABA_AR$ function (Fig. 3*B*). The charge swap (βE153K-βK196E) and double charge neutralization (βE153A-βK196A) shifted the GABA EC_{50} only by 37-

and 78-fold *vs*. the 2600- and 720-fold shifts predicted in the absence of an interaction (Table 1). Finally, mutant cycle analysis yielded a significant interaction energy of ≈1.4 kcal/mol (Fig. 4*A*). Charged residues at position β153 and β196 are conserved across all species and subtypes of the $GABA_AR$ β-subunit (Fig. 1*B*) supporting the idea that these residues are critical for $GABA_AR$ function.

While our data indicate that βE153 and βK196 are energetically coupled, the different fold changes in GABA EC_{50} upon mutating βE153 and βK196 (Table 1) together with the partial recovery in GABA EC_{50} of the charge swap (Fig. 2*B*, Table 1) indicate a more complex role than a simple electrostatic interaction and suggest that these residues are part of a larger network of interacting residues. βE153 is located near GABA binding site residues βE155 and βR207, which we previously identified are critical for GABA binding and gating (29, 30). We speculate that mutating βE153 is not only eliminating an interaction with K196 but is also affecting βE155 and βR207, hence the larger changes in GABA EC_{50} when βE153 was mutated as compared to K196 and the partial recovery in GABA EC_{50} of the charge swap. GABA binding and channel activation likely involves a dynamic interplay of these residues near the binding site. Because mutations at βE153 and βK196 increase GABA EC_{50}, the electrostatic interaction between βE153 and βK196 is likely part of the mechanism that stabilizes a ligand-bound receptor state. PB does not bind in the GABA binding site and mutating βE155 or βR207 has minimal affects on PB activation (29, 30); this likely explains why mutations at βE153 and βK196 have smaller effects on PB EC_{50} and the charge swap completely restores PB EC_{50}.

Findings in the nAChR support our conclusions that βE153 and βK196 play an important role in $GABA_AR$ activation. Mukhtasimova *et al.* (11) identified an electrostatic interaction between α1K145 (aligned with βE153) on β7 and α1Y190 (aligned with βK196) on β9 in the nAChR important for stabilizing the open state of the receptor, whereas in the unliganded-resting state an interaction between α1K145 and α1D200 (aligned with βR207) occurred. Also, in agonist-bound AChBP (31), an H-bond between K139 and Y185 (aligned with βE153 and βK196) is seen. An H-bond link between loops B and C in the α4 nAChR was also identified to be important for stabilizing both open and desensitized states (32).

Loop C Mobility. Cysteine substitutions at β153 and β196 disulfide crosslinked in the closed state (Fig. 4*B*). In our homology model, the C^{β}-C^{β} distance between E153C and K196C in the resting unliganded state is 10Å (C^{β}-C^{β} for -S-S- bond is 4.6 Å). Our results indicate that, in the resting state, loop C of the GABA binding site is mobile and residues may move as much as 5 Å.

Disulfide trapping β7 and β9 close to each other resulted in a reduction in both GABA and PB gated currents. The volume and length of a cysteine side chain is smaller than glutamate and lysine. We speculate that the disulfide bond positions βE153C and βK196C too close and traps the outer β-sheets in a conformation that reduces their torsional flexibility. In a recent study, disulfide crosslinking residues K144 (aligned with E153) and T198 in loop C of the α7 nAChR reduced the ability of acetylcholine to activate the receptor (33).

If loop C is mobile in the closed unliganded state, what happens to this mobility during receptor activation? When examined in the presence of GABA or PB, crosslinking between βE153C and βK196C was decreased suggesting that loop C is less mobile in GABA and PB bound receptor states. Notably in AChBP, Shi *et al.* (7) using hydrogen-deuterium exchange mass spectrometry and Gao *et al.* (34) using solution NMR have shown a reduced mobility of loop C in the presence of agonist.

In conclusion, we identify a salt bridge between two conserved charged residues in β7 and β9 of the $GABA_AR$ β-subunit that is critical for receptor activation by orthosteric and allosteric $GABA_AR$ ligands. Crosslinking experiments not only confirm spatial proximity between E153 and K196 but also predict inherent protein flexibility within these outer β-strands. We envision that in the resting state, the loop C region of the GABA binding site is highly mobile. GABA binding might then bring an order to this entropic state by positioning βE153 and βK196 via electrostatic interactions that restrict the movement of loop C. This restriction of loop C is likely important for stabilizing a ligand-bound state of the receptor. It remains to be determined whether the two remaining cousins of the $GABA_AR$ within this superfamily, the GlyR and the $5HT_3R$ also share similar interactions within the outer β-strands.

Materials and Methods

Mutagenesis and Expression in Oocytes. Rat cDNAs encoding α1, β2, and γ2S subunits of the $GABA_AR$ were subcloned into the pUNIV vector (35). Mutant β2 subunits were created as previously described (36).

Oocyte Electrophysiology. *Xenopus* oocyte isolation and two electrode voltage clamp recordings on *Xenopus* oocytes were performed as previously described (36). Stock solution of 0.3% H_2O_2 (Fisher Scientific) in ND96 buffer was prepared daily.

Concentration–Response Analysis. GABA concentration–response analyses were performed as described previously (36). PB concentration responses for WT and mutant receptors were performed either with or without a low PB concentration (EC_{5-30}) to correct for the drift in I_{PB} over the course of the experiment. Currents induced by each test concentration were normalized to the corresponding low PB concentration (where applicable) before curve fitting. The curve fits for PB concentration responses for the two methods were not significantly different and data were pooled for statistical analysis. At high micromolar concentrations and above, PB blocks $GABA_AR$. Relief of channel block upon drug wash yields a characteristic tail current. For PB concentration response curves, currents measured at high micromolar concentrations and above included tail current measurements. Nonlinear regression analysis was performed using GraphPad Prism 4 software.

Methanethiosulfonate (MTS) Modification of Substituted Cysteines. MTSES (methanethiosulfonate ethylsulfonate) [$CH_3SO_2SCH_2CH_2SO_3^-$] and MTSET (methanethiosulfonate ethyltrimethylammonium) [$CH_3SO_2SCH_2CH_2N(CH_3)_3^+$] (Biotium, Hayward, CA) were used to modify the introduced cysteines. Stock solutions were prepared as described previously (36). The effect of MTS modification was ascertained as follows: Oocytes expressing WT and mutant receptor were exposed to alternating low GABA (EC_{30-60}) and maximal GABA concentrations (defined by their respective GABA dose-response curves) spaced by a time interval that allowed full functional recovery. This protocol was continued until 2–3 successive current amplitudes in response to either concentration were stable. Stability was defined as ≤10% variation in current amplitudes. The average current amplitude from 2–3 stable GABA responses (low or maximal) was then calculated. Subsequently MTSET or MTSES at 2 mM was applied for 2 min followed by a 5- to 6-min wash. Following MTS application, oocytes were exposed to the same low and maximal GABA concentration and stabilized as described before. The average current amplitude from 2–3 stable GABA responses post-MTS application was again calculated. The effect of MTS application was calculated as follows: $[((I_{after}/I_{initial}) - 1) \times 100]$ where $I_{initial}$ and I_{after} are the averaged peak GABA currents (low or maximal) measured before and after MTS application, respectively.

Cysteine Cross-linking. Disulfide bond formation was induced by exposing oocytes expressing WT and mutant receptors to 0.3% H_2O_2 for 3 min followed by a 2- to 5-min wash. Effect of H_2O_2 oxidation on WT and mutant receptors was assayed by measuring the current amplitudes of GABA or PB responses before and after treatment. Oocytes were initially stabilized using EC_{50} GABA or PB concentration before exposure to H_2O_2. Stability was defined as ≤10% variation in the current amplitudes in response to two consecutive GABA or PB applications. The effect of H_2O_2 was calculated as follows: $[((I_{after}/I_{initial}) - 1) \times 100]$ where $I_{initial}$ and I_{after} are the stabilized peak GABA or PB currents measured before and after H_2O_2. Cysteine cross-linking in the presence of GABA or PB was ascertained using the same protocol as above except 300 mM GABA or 1 mM PB was applied in combination with H_2O_2. In all cases, the oocytes were washed sufficiently between drug applications to allow full functional recovery before testing the effect of H_2O_2. The reversibility of H_2O_2 effects was examined by exposing the oocytes to the reducing agent DTT (10

mM, 3 min) and measuring the current amplitudes of GABA and PB before and after DTT.

Statistical Analysis. LogEC_{50} values for GABA and PB concentration responses, changes in current amplitude in response to MTS application for low and maximal GABA concentration, and effects of DTT/H_2O_2 on single and double cysteine substitutions were analyzed using one-way ANOVA, followed by a post hoc Dunnett's test and/or a posthoc Bonferroni multiple comparison test to determine the level of significance between WT and mutant receptors.

Natural logarithm (ln) transformed values of WT and mutant EC_{50} values were used for computing interaction free energies, such that $\Delta\Delta G_{INT} = RT$ [ln(WT) + ln(mut1,mut2) − ln(mut1) − ln(mut2)], with propagated errors reported in standard error (SEM). $\Delta\Delta G_{INT} \pm$ error were analyzed using one-sample *t* test for statistical significance from zero energy, with degrees of freedom (df) = $N_{WT} + N_{MUT1} + N_{MUT2} + N_{MUT1,MUT2} - 4$, where N_X = number of EC_{50} experiments for WT or mutant receptors.

Structural Modeling. Homology modeling was performed as described previously (36).

ACKNOWLEDGMENTS. We thank Dr. Andrew J. Boileau for helpful discussions, Dr. Ken Satyshur for $GABA_AR$ homology modeling, and Say Thao for assistance with making the mutations. This work was supported by National Institutes of Health Grant NINDS 34727 (C.C.).

1. Sine SM, Engel AG (2006) Recent advances in Cys-loop receptor structure and function. *Nature* 440:448–455.
2. Farrant M, Nusser Z (2005) Variations on an inhibitory theme: Phasic and tonic activation of GABA(A) receptors. *Nat Rev Neurosci* 6:215–229.
3. Brejc K, *et al.* (2001) Crystal structure of an ACh-binding protein reveals the ligand-binding domain of nicotinic receptors. *Nature* 411:269–276.
4. Unwin N (2005) Refined structure of the nicotinic acetylcholine receptor at 4A resolution. *J Mol Biol* 346:967–989.
5. Henchman RH, Wang HL, Sine SM, Taylor P, McCammon JA (2005) Ligand-induced conformational change in the alpha7 nicotinic receptor ligand binding domain. *Biophys J* 88:2564–2576.
6. Gao F, *et al.* (2005) Agonist-mediated conformational changes in acetylcholine-binding protein revealed by simulation and intrinsic tryptophan fluorescence. *J Biol Chem* 280:8443–8451.
7. Shi J, Koeppe JR, Komives EA, Taylor P (2006) Ligand-induced conformational changes in the acetylcholine-binding protein analyzed by hydrogen-deuterium exchange mass spectrometry. *J Biol Chem* 281:12170–12177.
8. Hansen SB, *et al.* (2005) Structures of aplysia AChBP complexes with nicotinic agonists and antagonists reveal distinctive binding interfaces and conformations. *EMBO J* 24:3635–3646.
9. Lee WY, Sine SM (2005) Principal pathway coupling agonist binding to channel gating in nicotinic receptors. *Nature* 438:243–247.
10. Purohit P, Mitra A, Auerbach A (2007) A stepwise mechanism for acetylcholine receptor channel gating. *Nature* 446:930–933.
11. Mukhtasimova N, Free C, Sine SM (2005) Initial coupling of binding to gating mediated by conserved residues in the muscle nicotinic receptor. *J Gen Physiol* 126:23–39.
12. Amin J, Weiss DS (1993) $GABA_A$ receptor needs two homologous domains of the beta-subunit for activation by GABA but not by pentobarbital (see comments). *Nature* 366:565–569.
13. Akk G, Steinbach JH (2000) Activation and block of recombinant GABA(A) receptors by pentobarbitone: A single-channel study. *Br J Pharmacol* 130:249–258.
14. Karlin A, Akabas MH (1998) Substituted-cysteine accessibility method. *Methods Enzymol* 293:123–145.
15. Hidalgo P, MacKinnon R (1995) Revealing the architecture of a K^+ channel pore through mutant cycles with a peptide inhibitor. *Science* 268:307–310.
16. Faiman GA, Horovitz A (1996) On the choice of reference mutant states in the application of the double-mutant cycle method. *Protein Eng* 9:315–316.
17. Schreiber G, Frisch C, Fersht AR (1997) The role of Glu73 of barnase in catalysis and the binding of barstar. *J Mol Biol* 270:111–122.
18. Mercado J, Czajkowski C (2008) [Gamma]-aminobutyric acid (GABA) and pentobarbital induce different conformational rearrangements in the $GABA_A$ receptor α1 and β2 pre-M1 regions. *J Biol Chem* 283:15250–15257.
19. Horovitz A (1996) Double-mutant cycles: A powerful tool for analyzing protein structure and function. *Fold Des* 1:R121–126.
20. Sadovsky E, Yifrach O (2007) Principles underlying energetic coupling along an allosteric communication trajectory of a voltage-activated K^+ channel. *Proc Natl Acad Sci USA* 104:19813–19818.
21. Yifrach O, MacKinnon R (2002) Energetics of pore opening in a voltage-gated K(+) channel. *Cell* 111:231–239.
22. Careaga CL, Falke JJ (1992) Structure and dynamics of Escherichia coli chemosensory receptors. Engineered sulfhydryl studies. *Biophys J* 62:209–216.
23. Liu X, Alexander C, Serrano J, Borg E, Dawson DC (2006) Variable reactivity of an engineered cysteine at position 338 in cystic fibrosis transmembrane conductance regulator reflects different chemical states of the thiol. *J Biol Chem* 281:8275–8285.
24. Amin J (1999) A single hydrophobic residue confers barbiturate sensitivity to gamma-aminobutyric acid type C receptor. *Mol Pharmacol* 55:411–423.
25. Pistis M, Belelli D, McGurk K, Peters JA, Lambert JJ (1999) Complementary regulation of anaesthetic activation of human (alpha6beta3gamma2L) and Drosophila (RDL) GABA receptors by a single amino acid residue. *J Physiol* 515(Pt 1):3–18.
26. Serafini R, Bracamontes J, Steinbach JH (2000) Structural domains of the human $GABA_A$ receptor 3 subunit involved in the actions of pentobarbital. *J Physiol* 524(Pt 3):649–676.
27. Gruia AD, Fischer S, Smith JC (2004) Kinetics of breaking a salt-bridge critical in protein unfolding. *Chem Phys Lett* 385:337–340.
28. Sheldahl C, Harvey SC (1999) Molecular dynamics on a model for nascent high-density lipoprotein: Role of salt bridges. *Biophys J* 76:1190–1198.
29. Newell JG, McDevitt RA, Czajkowski C (2004) Mutation of glutamate 155 of the GABAA receptor beta2 subunit produces a spontaneously open channel: A trigger for channel activation. *J Neurosci* 24:11226–11235.
30. Wagner DA, Czajkowski C (2001) Structure and dynamics of the GABA binding pocket: A narrowing cleft that constricts during activation. *J Neurosci* 21:67–74.
31. Celie PH, *et al.* (2004) Nicotine and carbamylcholine binding to nicotinic acetylcholine receptors as studied in AChBP crystal structures. *Neuron* 41:907–914.
32. Grutter T, *et al.* (2003) An H-bond between two residues from different loops of the acetylcholine binding site contributes to the activation mechanism of nicotinic receptors. *EMBO J* 22:1990–2003.
33. McLaughlin JT, Fu J, Sproul AD, Rosenberg RL (2006) Role of the outer beta-sheet in divalent cation modulation of alpha7 nicotinic receptors. *Mol Pharmacol* 70:16–22.
34. Gao F, *et al.* (2006) Solution NMR of acetylcholine binding protein reveals agonist-mediated conformational change of the C-loop. *Mol Pharmacol* 70:1230–1235.
35. Venkatachalan SP, *et al.* (2007) Optimized expression vector for ion channel studies in Xenopus oocytes and mammalian cells using alfalfa mosaic virus. *Pflugers Arch* 454:155–163.
36. Mercado J, Czajkowski C (2006) Charged residues in the alpha1 and beta2 pre-M1 regions involved in $GABA_A$ receptor activation. *J Neurosci* 26:2031–2040.